AEM
Journals.ASM.org

Metabolome and Transcriptome of the Interaction between *Ustilago maydis* and *Fusarium verticillioides In Vitro*

Wilfried Jonkers,[a] Alma E. Rodriguez Estrada,[b]* Keunsub Lee,[b]* Andrew Breakspear,[a]* Georgiana May,[b] and H. Corby Kistler[a,c]

Department of Plant Pathology, University of Minnesota, Saint Paul, Minnesota, USA[a]; Department of Ecology, Evolution and Behavior, University of Minnesota, Saint Paul, Minnesota, USA[b]; and USDA ARS, University of Minnesota, Saint Paul, Minnesota, USA[c]

The metabolome and transcriptome of the maize-infecting fungi *Ustilago maydis* and *Fusarium verticillioides* were analyzed as the two fungi interact. Both fungi were grown for 7 days in liquid medium alone or together in order to study how this interaction changes their metabolomic and transcriptomic profiles. When grown together, decreased biomass accumulation occurs for both fungi after an initial acceleration of growth compared to the biomass changes that occur when grown alone. The biomass of *U. maydis* declined most severely over time and may be attributed to the action of *F. verticillioides*, which secretes toxic secondary metabolites and expresses genes encoding adhesive and cell wall-degrading proteins at higher levels than when grown alone. *U. maydis* responds to cocultivation by expressing siderophore biosynthetic genes and more highly expresses genes potentially involved in toxin biosynthesis. Also, higher expression was noted for clustered genes encoding secreted proteins that are unique to *U. maydis* and that may play a role during colonization of maize. Conversely, decreased gene expression was seen for *U. maydis* genes encoding the synthesis of ustilagic acid, mannosylerythritol D, and another uncharacterized metabolite. Ultimately, *U. maydis* is unable to react efficiently to the toxic response of *F. verticillioides* and proportionally loses more biomass. This *in vitro* study clarifies potential mechanisms of antagonism between these two fungi that also may occur in the soil or in maize, niches for both fungi where they likely interact in nature.

Fungi that infect plants modulate the plant immune response and by doing so define the nature of that interaction. All fungi possess molecular signals, such as ergosterol (9), chitin (8) or glycosylated peptides (3), which can cause the plant to initiate a defensive immune response that is the basis for nonhost resistance (11). Pathogenic fungi produce additional effector molecules, often small secreted peptides, which circumvent this basic immune response, allowing for greater fungal colonization and reproduction (21). Many fungi, however, reside within plants without producing disease as biotrophic endophytes and may establish mutualistic interactions. For example, arbuscular mycorrhizal (AM) fungi mobilize soil nutrients for the plant in exchange for products of photosynthesis, and these fungi also employ effector-driven suppression of the nonhost resistance response (15).

Plants harbor a wide range of endophytes in addition to AM fungi. These fungi may confer fitness benefits, such as increased plant biomass, drought tolerance, or adaptation to specific environments (24). The plant microbiome is only now beginning to be described (12). Clearly, plant-inhabiting fungi not only must cope with host defenses which are capable of shaping the fungal community (27) but also must coexist with other fungi within the plant. Interactions between endophytic fungi may potentially limit growth through antibiosis, such as by secreting toxic antifungal secondary metabolites or by competition for nutrients, such as by the sequestration of iron by siderophore-producing fungi (16).

We have chosen the maize-inhabiting fungi *Ustilago maydis* and *Fusarium verticillioides* as models for studying the molecular basis for fungal interactions *in planta* and in soil. *U. maydis* is a dimorphic basidiomycetous fungus that causes corn smut disease on maize. *F. verticillioides*, often considered solely as an ear and stalk rot pathogen of maize, is also a persistent endophytic fungus that can systemically infect maize without producing disease symptoms (2, 22). *F. verticillioides* has been shown to reduce disease severity caused by *U. maydis* in maize, and so this fungus-fungus interaction may be critical for understanding corn smut pathogenesis and its consequences in nature (18). Previously, we have focused on differences in metabolic profiles between the two species grown *in vitro* in single cultures and in cocultures in an effort to understand how accumulation of small molecules may affect this interaction (23). For the current work, we extend and broaden this investigation by determining changes in transcript profiles that occur during cocultivation and by establishing links between gene expression changes, changes in metabolic profiles, and the consequences for growth during the fungus-fungus interaction.

MATERIALS AND METHODS

Fungal inoculations. One isolate of *F. verticillioides* and two compatible *U. maydis* haploids were used in this experiment. *U. maydis* U18 mating type a_2b_{11} and C7 mating type a_1b_{12} and *F. verticillioides* isolate NRRL 20956 were acquired from the May Lab fungal collection and the Agricultural Research Service Culture collection, respectively. The *F. verticillioides* isolate has been fully sequenced (20), behaves as an endophyte under greenhouse experiments (18), and has been used previously to study *in vitro* fungal interactions (23).

Received 12 December 2011 Accepted 28 February 2012
Published ahead of print 9 March 2012
Address correspondence to H. Corby Kistler, hckist@umn.edu.
* Present address: Alma E. Rodriguez Estrada, Department of Natural and Applied Sciences, University of Wisconsin-Green Bay, Green Bay, Wisconsin, USA; Keunsub Lee, Center for Plant Transformation, Iowa State University, Ames, Iowa, USA; Andrew Breakspear, John Innes Centre, Norwich Research Park, Norwich, United Kingdom.
Supplemental material for this article may be found at http://aem.asm.org/.

doi:10.1128/AEM.07841-11

F. verticillioides and *U. maydis* haploids were grown separately in sterilized potato dextrose broth medium (50 ml) contained in 250-ml flasks (3 days, 25°C). *F. verticillioides* cultures were filtered over two layers of sterilized Miracloth, and the filtrate was centrifuged at 4,000 rpm for 5 min to collect spores. The resulting pellet was washed three times, and the spore concentration was adjusted to yield a total of 10^7 spores in 100 μl of water (23). *U. maydis* cultures were centrifuged at 4,000 rpm, the resulting sporidium pellet was washed three times, and sporidium concentration was adjusted to yield 5×10^6 *U. maydis* sporidia in 50 μl of sterile/distilled water. Both *U. maydis* haploids were mixed together previous to medium inoculation. Fungi were individually inoculated or cocultivated in 50 ml of sterilized Czapek-Dox broth medium (CDB) contained in 250-ml Erlenmeyer flasks. The cultures were incubated in darkness at 27°C in a shaker incubator at 150 rpm (New Brunswick floor incubator).

A total of four treatments (*F. verticillioides* alone, *U. maydis* alone, *F. verticillioides* and *U. maydis* together, and no fungus) were included in these experiments. For the transcriptomics assays, only three treatments (*F. verticillioides* alone, *U. maydis* alone, *F. verticillioides* and *U. maydis* together) were analyzed, with *F. verticillioides* alone and *U. maydis* alone serving as each other's background control. Three replicates of each treatment were used.

Biomass sampling and quantification. For absolute biomass measurements, separate duplicate samples of each treatment were harvested at days 1, 2, 3, 5, and 7. *F. verticillioides* and cocultivated cultures were filtered over two layers of Miracloth, the filtrate was placed in 50-ml Falcon tubes, and fungal cells were pelleted by centrifugation (4,000 rpm). *U. maydis* cultures were transferred to 50-ml falcon tubes, and sporidia were pelleted by centrifugation (4,000 rpm). Collected spores, sporidia, and mycelium were lyophilized and weighed.

Relative changes in the DNA content and inferred biomass for each fungal species were measured using real-time PCR. From *F. verticillioides*, both mycelium and spores from each replicate were combined and finely ground with liquid nitrogen in a frozen mortar and pestle. Approximately 20 mg of fungal tissue was placed in frozen microcentrifuge tubes (1.5 ml) and stored at −80°C until use. *U. maydis* sporidia pellets were finely ground and stored as detailed above. The fungal tissue weight used for DNA extractions was recorded and used to normalize data obtained from real-time PCR assays.

DNA was extracted from the ground fungal tissue using the OmniPrep kit for fungi by following the manufacturer's instructions (GBiosciences). The DNA was suspended in Tris-EDTA buffer and stored at −80°C upon use. Species-specific primers and labeled probes (TaqMan) for *F. verticillioides* (FusqPCR_F, FusqPCR_R, and Fusca-VIC) and *U. maydis* (Emt1qPCR_F, Emt1qPCR_R, and UMemt1–6-carboxyfluorescein [FAM]) were used in multiplex reactions by following the protocols and real-time PCR settings described in reference 23. Data obtained from real-time PCR (corresponding to the number of genome equivalents) was normalized to the weight of the fungal tissue used for DNA extraction.

Metabolite sampling and measurement. For metabolite extraction, the supernatant from liquid cultures (fungal cells removed) was placed in 50-ml Falcon tubes. Two milliliters of the supernatant was mixed with 2 ml of methanol (≥99.9%; Sigma-Aldrich) acidified with formic acid (1:0.01, vol/vol). Samples were placed in an ultrasonic bath (Mettler Electronics) for 90 min. Then, two volumes of 1.5 ml of the extracts each were placed in 2-ml microcentrifuge tubes and dried in a speed vacuum (SpeedVac SC100; Savant) for 6 h. The dried pellets were stored at 4°C for less than 1 week before analysis. The dried pellets were ultrasonically resuspended with 500 μl of acidified methanol (1:0.001, methanol/formic acid). Metabolites were analyzed using an ultra-performance liquid chromatography/time-of-flight mass spectrometer instrument (Acquity chromatograph attached to an LCT Premier XE Micromass spectrometer [Waters]). The protocols used for metabolite analysis and data processing were performed as described earlier (23). In short, data were acquired, visualized, and processed using the MassLynx software (version 4.1; Waters). Individual chromatographic peaks were manually extracted from the profiles, and peak areas were automatically calculated. For each sample, the peak areas were normalized to the dry weight of the sample, giving peak areas/mg (dry weight) as direct estimates of each compound's concentration. Therefore, peak areas/mg (dry weight) were compared over time and across treatments in order to elucidate relative changes in metabolite concentrations.

Fusaric acid growth inhibition experiment. *U. maydis* strains were grown in potato dextrose broth (PDB) for 2 days, and the sporidial density was determined using a hemocytometer. *U. maydis* sporidia were resuspended in fresh PDB to the final concentration of 10^8 cells/ml and diluted to the concentration of 2×10^5 cells/ml in a 50-ml conical tube containing 5 ml fresh PDB. Fusaric acid (molecular weight [MW] = 179.22) was dissolved in 100% ethanol to a concentration of 20 mg/ml. To determine if fusaric acid inhibits *U. maydis* growth, it was added to the PDB in concentrations of 10, 20, 30, 50, and 100 μg/ml. As a control, ethanol alone was added to PDB to a percentage of 0.5%. *U. maydis* sporidial growth was monitored daily for 3 days using a hemocytometer.

Gene expression analysis. RNA was extracted from frozen and ground fungal tissue using the TRIzol reagent (Invitrogen) method according to the manufacturer's protocol. RNA quality was assessed with gel electrophoresis, and RNA cleanup was done using the RNAeasy minikit (Qiagen) prior to microarray labeling. RNA labeling reactions were performed according to the standard Affymetrix protocols. The samples were used to query a custom Affymetrix GeneChip microarray constructed with probe sets representing predicted genes for *U. maydis* strain 521 (13) and *F. verticillioides* NRRL 20956 (20). Gene models used for the array were from the manually annotated *U. maydis* calls at MUMDB (http://mips.helmholtz-muenchen.de/genre/proj/ustilago/index.html) and the second *F. verticillioides* annotation available at the Broad Institute's Fusarium Comparative Genomes website (http://www.broadinstitute.org/annotation/genome/fusarium_graminearum/MultiHome.html). Information of these chips can be found at the PLEXDB site (http://www.plexdb.org/plex.php?database=Fungus). Hybridizations were performed at the BioMedical Genomics Center of the University of Minnesota. CEL files were imported in Refiner 5.3 software (Expressionist), and robust multichip average (RMA) preprocessing was applied. Signal values ($P = 0.04$) obtained in the Analyst software (Expressionist) were normalized to the median. Fold expression filters were applied as described in Results. Microarray data files are available at the PLEXdb expression database (6) as experiments NF3 (*U. maydis* probes) and NF4 (*F. verticillioides* probes).

RESULTS

Biomass quantification. Cocultivation of *U. maydis* and *F. verticillioides* in CDB greatly affects biomass accumulation of the two fungi. When the two fungi are grown separately (Fig. 1A, solid black and solid gray lines), rapid growth is observed over a period of 3 days until a stationary phase is reached that continues until the end of the experiment. During cocultivation, however, total biomass increases more rapidly than in single culture over the first 2 days and then reaches a stationary phase at day 2 (Fig. 1A, dashed black line). The total biomass during cocultivation stays relatively constant after 2 days and is less than that expected from adding together each species' biomass observed in single culture (Fig. 1A, dashed gray line) and even lower than when *F. verticillioides* is grown alone.

The relative percentage of the two fungal genomes during cocultivation was measured using quantitative PCR (qPCR). The genomic share of *F. verticillioides* in cocultivation treatments increases over time as the share of *U. maydis* diminishes (Fig. 1B). This is partly due to the enhanced biomass accumulation capacity of *F. verticillioides* as seen in the biomass curve. Still, while the decline of the *U. maydis* genomic share continues after 3 and 5 days as it does in the single-inoculation cultures, the total fungal

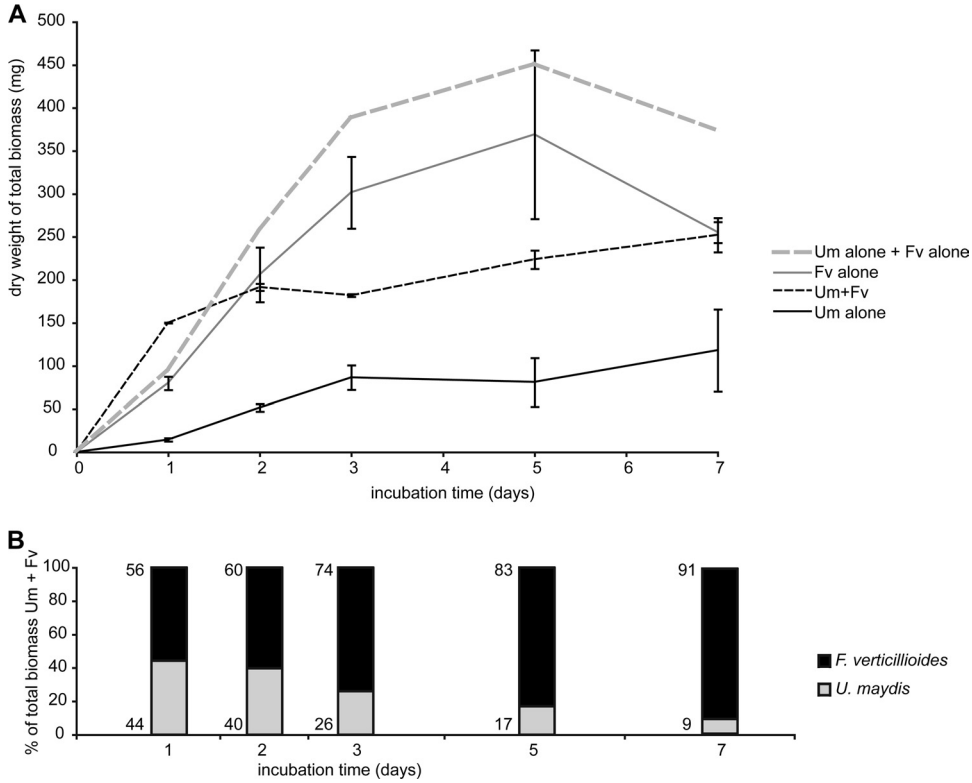

FIG 1 (A) Total dry biomass weight of single and cocultivated cultures measured at different time points. The upper dashed gray line represents the sum of the biomasses of *F. verticillioides* and *U. maydis* grown alone. The dotted gray line, second from top, represents the biomass of *F. verticillioides* alone. The dashed black line represents the biomasses of *F. verticillioides* and *U. maydis* grown together. The lower black line represents the biomass of *U. maydis* grown alone. (B) Percentage of each fungus in the cocultivation samples at different time points measured by the qPCR technique. Percentages of both fungi at each time point are given in the upper and lower left of the bar for *F. verticillioides* and *U. maydis*, respectively.

biomass stays more or less stable (Fig. 1A). All together, results for qPCR and biomass accumulation suggest that cocultivation limits the growth of both *F. verticillioides* and *U. maydis*, although growth of *U. maydis* is more strongly limited compared to growth of *F. verticillioides*.

Metabolite profiles. Metabolite profiles were visually examined, and chromatographic peaks detected in the negative control (liquid medium inoculated with water) were removed from further analysis. The concentration of the metabolite was calculated by dividing the peak area by the average biomass weight of each sample. Using this method of calculation, in the cocultivated samples, the concentrations of the metabolites per total biomass are lower than if grown alone, since only a fraction of the total biomass in mixed cultures is of the species actually producing the metabolite.

A total of 10 chromatographic peaks corresponding to fungal metabolites were detected across the experiment. Three chromatographic peaks were specifically detected in *F. verticillioides* samples and seven in *U. maydis* samples (Table 1).

Nine of the 10 chromatographic peaks were detected previously (23) in an *in vitro* study performed on solid medium. These metabolites include ustilagic acid (UA) from *U. maydis*, fusaric acid (FA) from *F. verticillioides*, and unidentified peaks from both fungi. In the previous studies using solid media (23, 32), metabolites were extracted using toluene, which is an extraction protocol different than that used here. In that study, 17 other peaks were identified that were not found in this study, among them mannosylerythritol lipid (MEL) D from *U. maydis* and fumonosins B1 and B2 and bikaverin from *F. verticillioides*. The apparent absence of fumonosins and bikaverin may also be explained by the fact that in the previous study these metabolites were found only on potato dextrose agar (PDA) and not on Czapek-Dox agar (CDA). Still, we choose to use CDB in this study because fusaric acid is produced on CDA and not in PDA (22). One new unidentified peak, Fv3, was found in cultures inoculated with *F. verticillioides* but was not previously found in the solid-medium study.

***F. verticillioides* metabolites.** The concentration of fusaric

TABLE 1 Metabolites from *F. verticillioides* and *U. maydis* determined in the supernatant of single and cocultivation cultures

Fungus	Peak ID	*m/z*[a]	Metabolite ID[b]
F. verticillioides	Fv1	180.100	Fusaric acid
	Fv2	495.207	Unidentified
	Fv3	602.441	Unidentified
U. maydis	Um1	461.160	Unidentified
	Um2	489.191	Unidentified
	Um3	807.419	Ustilagic acid B
	Um4	819.439	Ustilagic acid A
	Um5	775.411	Ustilagic acid derivate
	Um6	803.442	Ustilagic acid derivate
	Um7	643.330	Unidentified

[a] Mass-to-charge ratio (*m/z*) of the most intense ion in the spectrum.
[b] Putative identification based on the mass-to-charge ratio of the most intense ion in the spectrum (23).

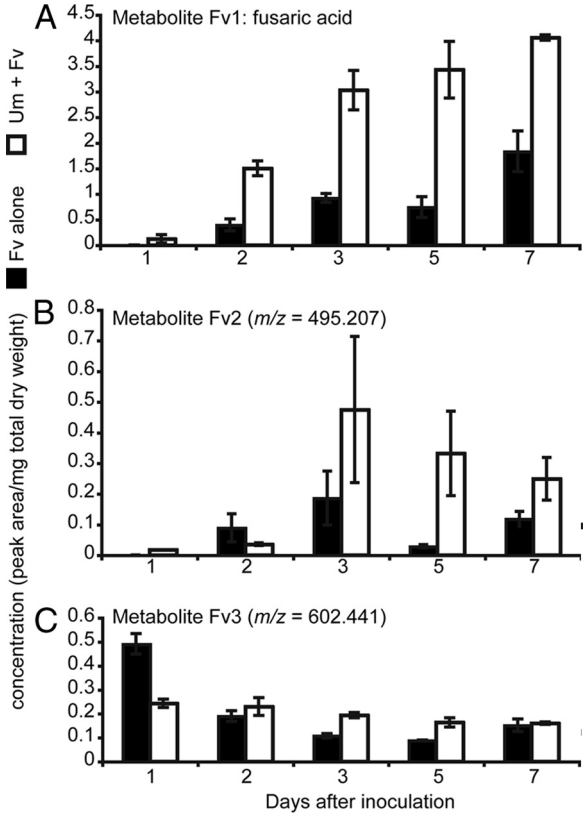

FIG 2 Histograms of fusaric acid (metabolite Fv1) and *F. verticillioides* metabolites Fv2 and Fv3 determined in single and cocultivation cultures at different time points. Black bars represent single-grown *F. verticillioides* samples and white bars the cocultivated *F. verticillioides* and *U. maydis* samples.

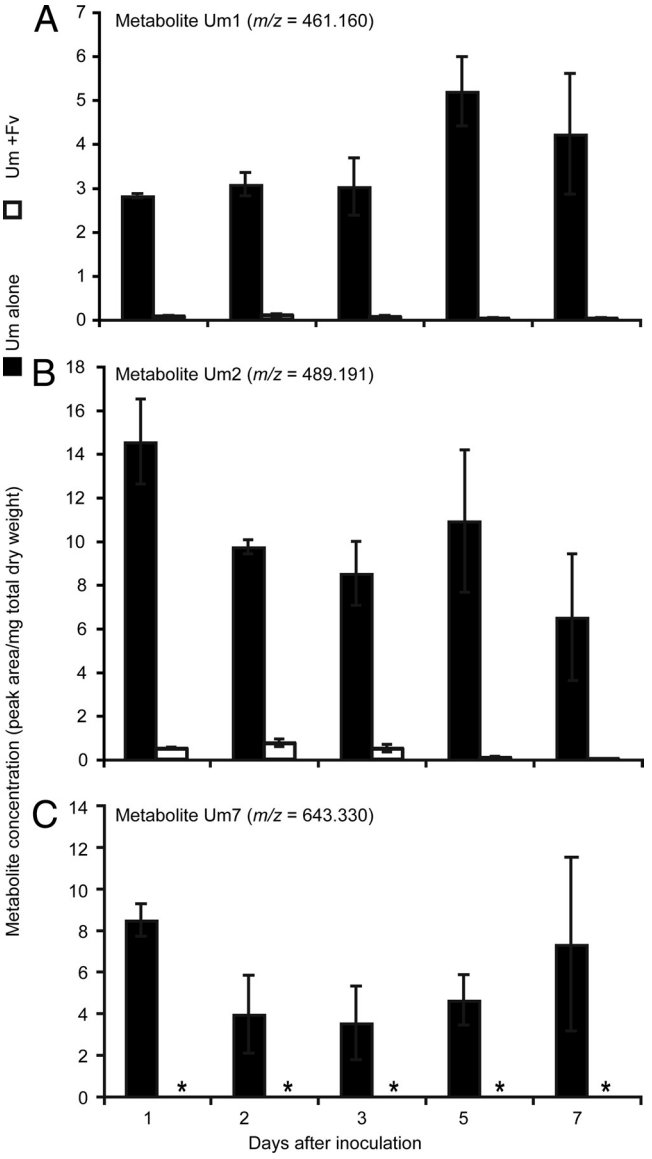

FIG 3 Histograms of *U. maydis* metabilites Um1, Um2, and Um7 determined in single and cocultivation cultures at different time points. *, no metabolite peak detected. Black bars represent single-grown *U. maydis* samples and white bars the cocultivated *F. verticillioides* and *U. maydis* samples.

acid (metabolite Fv1) produced by *F. verticillioides* increases over time when *F. verticillioides* was grown alone. However, even higher concentrations of this compound were detected in cocultivated cultures (Fig. 2A). *F. verticillioides* metabolite Fv2 is detected at day two, and its concentration varies over time in single cultures. During cocultivation, its concentration increases between day 1 and day 3 and then declines again. A higher concentration of this metabolite than that of single cultures is present in cocultivation samples from days 3 to 7 (Fig. 2B). Metabolite Fv3 concentration declines over time from days 1 to 5 but increases slightly at day 7 compared to that in single cultures. Cocultivation seems to suppress the decline of this metabolite, especially at days 3 and 5 (Fig. 2C).

***U. maydis* metabolites.** Concentrations of unidentified metabolites Um1, Um2, and Um7 are much lower in cocultivation than during growth alone and appear to be strongly inhibited during cocultivation (Fig. 3). In single cultures, each detected metabolite is present at all time points at a roughly constant concentration. Metabolite Um1 and Um2 concentrations are significantly lower (30- to 40-fold) after 1 day of cocultivation than for growth alone and almost disappear after days 5 to 7 (Fig. 3A and B). The concentration of metabolite Um7 is high during the first day of the single-culture growth and decreases slightly later in the experiment. This metabolite is below detectable levels in cocultivated cultures (marked with asterisks in Fig. 3C), though larger amounts of this metabolite were detected previously during cocultivation on PDA medium (23).

The glycolipid ustilagic acid was detected mostly in cultures of *U. maydis* grown alone. Concentrations of metabolites E (ustilagic acid B), J (ustilagic acid A), and K and and L (ustilagic acid derivatives) in *U. maydis* grown alone seem to be more or less constant at all time points. However, the concentrations are significantly lower in cocultivated samples at days 1 and 2 and are not detected after day 3 or later (Fig. 4A). Because the gene cluster for ustilagic acid synthesis has been identified (32), gene expression from this cluster can be correlated with metabolite concentration (below).

Gene expression analysis. Gene expression was determined at days 2 and 5 after inoculation using a fungal microarray having predicted genes from *F. verticillioides* and *U. maydis*. Since during cocultivation the RNA of each fungal strain is only a fraction of the total RNA, the expression value of genes during cocultivation will appear lower than values of the same genes expressed in cultures of

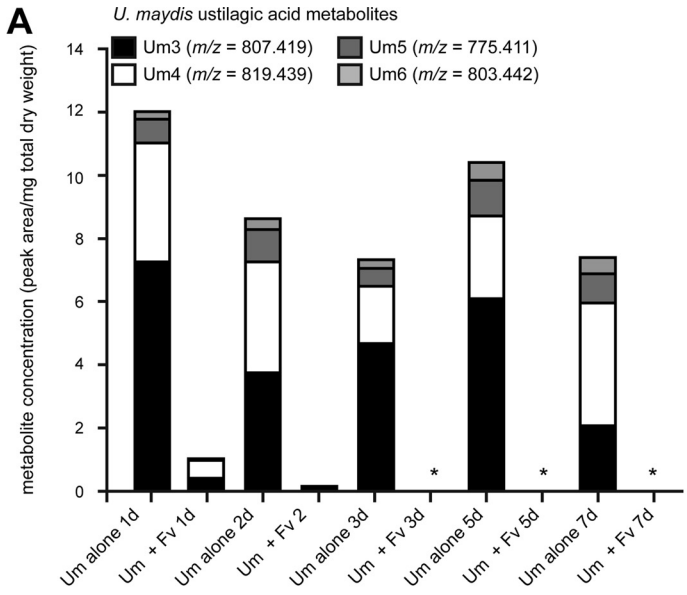

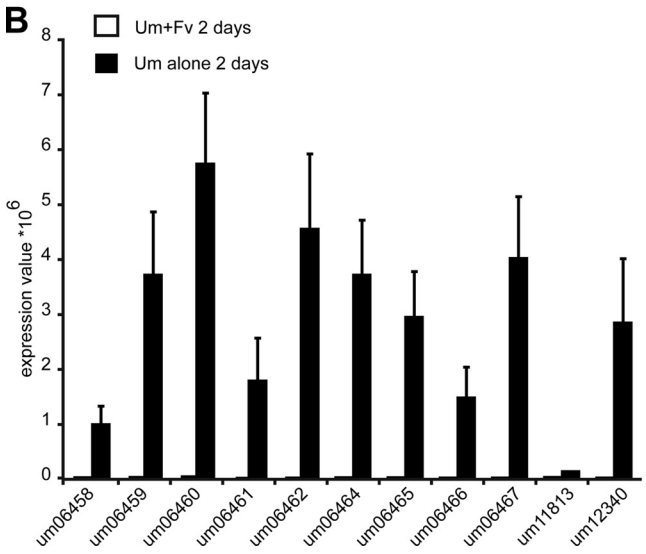

Locus ID	gene[1]	Putative function
um06458	*rua1*	Transcriptional regulator of ustilagic acid biosynthetic genes
um06459	*cyp2*	ω-1 hydroxylation of 16-OH palmitic acid
um06460	*fas2*	Synthesis of long- and/or short -chain fatty acid
um06461	*atr1*	Export of UA
um06462	*uat1*	Acetylation/acylation of cellobiose
um06463	*cyp1*	ω-Hydroxylation of palmitic acid
um06464	*orf1*	Unknown
um06465	*orf2*	Unknown
um06466	*uhd1*	Hydroxylation of short chain fatty acid
um06467	*ugt1*	Glycosylation of 16-OH palmitic acid
um11813	*orf3*	Unknown
um12340	*ahd1*	α-Hydroxylation of palmitic acid

FIG 4 (A) Histogram of *U. maydis* ustilagic acid metabolite peaks determined in single and cocultivation cultures at different time points. Bars are composed of the ustilagic acid metabolites presented in different colors: black is metabolite Um3, white is metabolite Um4, dark gray is metabolite Um5, and light gray is metabolite Um6. *, no metabolite peak detected. (B) Histogram of expression values of the genes from the ustilagic acid cluster in single and cocultivation cultures 2 days after inoculation. Black bars represent single-grown *U. maydis* samples and white bars the cocultivated *F. verticillioides* and *U. maydis* samples. The table on the left gives the gene names and putative function for the encoded proteins found in the cluster. [1], gene and annotated function are as mentioned previously (32).

each fungus grown alone. From the qPCR determinations of DNA content, the relative abundance of *F. verticillioides* to *U. maydis* was approximated to be 60:40 after 2 days and 80:20 after 5 days. However, because we cannot correlate the genomic ratios directly to mRNA ratios, we chose not to correct for these values. Due to the above-described considerations, we examined only genes that demonstrated ≥2-fold-increased expression during cocultivation compared to that of single cultivation and focused on genes that function within gene clusters. Most changes in gene expression are especially pronounced after 2 days rather than 5 days. It is possible that the changes in gene expression are more easily observed when the fungi are still growing in an exponential phase at 2 days and less when the growth has slowed down to a stationary phase at 5 days. Another explanation can be that the interaction is different at days 2 and 5.

***U. maydis* gene clusters differentially expressed during cocultivation. (i) Ustilagic acid.** Gene expression responsible for ustilagic acid biosynthesis seems to be completely absent in the cocultivation samples compared to the high expression levels observed for each gene from the cluster at day 2 in single cultures of *U. maydis* (Fig. 4B). The shutdown of the ustilagic acid biosynthetic cluster corresponds to results for the metabolite profile (Fig. 4A) and suggests that cocultivation with *F. verticillioides* inhibits expression of the genes required for ustilagic production by *U. maydis*.

(ii) Mannosylerythritol lipid. Even though we could not de-

tect the metabolite MEL in the liquid culture with the sampling techniques we used, we did find expression of genes involved in MEL biosynthesis (10). As seen with ustilagic acid, expression of the genes involved in MEL biosynthesis is detected in single cultures after 2 days but almost completely absent in cocultivation cultures (Fig. 5A). This suggests that cocultivation with *F. verticillioides* also inhibits expression of the genes required for MEL production by *U. maydis*.

(iii) Ferrichrome and ferrichrome A. *U. maydis* actively responds to cocultivation with *F. verticillioides* by the expression of gene clusters containing genes involved in uptake of essential nutrients and defense-related genes. Genes involved in the biosynthesis of the siderophores ferrichrome and ferrichrome A (34) are upregulated during cocultivation at 2 days (Fig. 5B). Two genes encoding siderophore peptide synthases, *fer3* (um01434) and *sid2* (um10189), especially show high expression levels during cocultivation compared to those of single cultures.

Additionally, we found different expressions of genes that reside in two putative clusters called msum_10 and msum_11 (19). Cluster msum_10 consists of 10 genes and was identified by one cooccurring motif seed found in the promoter sequences (19). The cluster includes genes encoding a polyketide synthase (PKS) protein identified earlier (4), a secreted protein (um10536), and proteins with different functions (Fig. 5D). All 10 genes from the cluster are expressed at lower levels during cocultivation than with single cultures. Expression is not completely shut down as seen with the UA and Mel D clusters, but a significant decrease of expression is seen for several genes from the cluster.

Cluster msum_11 encompasses 17 genes and was identified by three cooccurring motif seeds found in the promoter sequences (19). The cluster includes genes encoding PKS proteins (um04095 and um04097), a protein related to versicolor B synthase (um11112), another PKS protein (um04105), an *O*-methyltransferase (um04106), a cytochrome p450 (um04109), a flavin adenine dinucleotide (FAD)-binding monooxygenase (um04107), a multicopper oxidase (um11111), and two predicted transcription factors (um11110 and um04101) (Fig. 5C). Seven of these genes show slightly higher expression levels during cocultivation than in single cultures. Also, three *U. maydis*-specific genes are among these (um4098, um04104, and um12253), although low expression levels are found for all three.

Whether either cluster actually produces a secondary metabolite, the identity of the products, and the conditions under which these compounds are produced are not yet known.

Other *U. maydis* genes differently expressed during cocultivation. After 2 and 5 days in culture, 70 and 39 genes, respectively, from *U. maydis* were more highly expressed (≥2-fold) during cocultivation with *F. verticillioides* than when grown alone (see Data Set S1 in the supplemental material). In addition to the genes involved in iron uptake via siderophore production, the um11950 gene, also predicted to be involved in siderophore iron transport, is upregulated during cocultivation at day 2.

Genes encoding multidrug resistance proteins and enzymes that often play a role in breakdown or alteration of toxic compounds were found upregulated during cocultivation. These include um05642, a gene encoding probable multidrug-resistant transporter Snq2 from yeast (7); um03976, a gene encoding a drug resistance protein related to Pdr16 from yeast (33); and um00034, a gene encoding another probable multidrug resistance transporter. Also, um00205, encoding the heat shock protein Hsp12, and um05507, encoding the oxidoreductase general stress protein 39, were upregulated. Two genes that are upregulated at day 2 are also upregulated after 5 days: um00384, encoding an unknown protein, and um10233, a conserved hypothetical *Ustilago*-specific protein. Also, genes encoding a hydrophobin (um04433), a metallothionein (um11921), and a protein related to the transcription factor Rds1 (26) from yeast (um00395) are found upregulated.

Besides um10233, genes specific for *Ustilago* spp. and the *Ustilaginaceae* were found to be upregulated at days 2 and 5. Among them are genes that are considered *U. maydis* specific or weakly conserved among related *Ustilago* species and with annotation at nonsyntenic regions at chromosome ends (see Table S1 in reference 28). Three of such genes are more highly expressed in cocultivation compared to in growth alone (see Data Set S1 in the supplemental material): after 5 days, um06509, encoding a protein related to phenylalanine ammonia-lyase, and after 2 days, three genes encoding proteins from the possible gene cluster described in Fig. 5C (um04095, um04097, and um11111).

Genes listed in Table S2 of reference 13 as members of expanded families in the *U. maydis* genome were also upregulated after 5 days in cocultivation compared to in growth alone (see Data Set S1 in the supplemental material): um01392 (family 18, questionable open reading frames [ORFs] in repetitive regions), um03558 (family 3, similarly expanded in other *Basidiomycota*), and um05528 (family 14, similarly expanded in *Basidiomycota* and *Ascomycota*).

Genes for secreted proteins are clustered (13) and are upregulated during cocultivation (see Table S6 in reference 13). Also upregulated are genes identified in variable genome regions detected by comparing *U. maydis* and another corn smut fungus, *Sporosorium reilianum* (see Table S5 in reference 28). After 2 days, um01885, um02191, um02295 (reassigned as um10070, encoding a benzoate-4-monooxygenase), um02535, um03747, um05305, um10233, and um10556 were found upregulated during cocultivation compared to in growth of *U. maydis* alone. After 5 days, um00792, um00445, um01455, um02537, um02854, um05302, um05312, um10233, and um10500 were found upregulated during cocultivation compared to in growth alone (see Data Set S1 in the supplemental material). No function is known for these genes, and typically they are upregulated coordinately with other genes from the cluster during tumor development (13). We speculate that these genes may encode proteins involved in the defense against other microbes during *in planta* colonization.

The gene sets showing 2-fold-higher expression were imported into the functional category (FunCat) database directory of MIPS (25) in order to determine if the genes differentially regulated during cocultivation are significantly enriched in particular gene categories compared to the genome as a whole ($P < 0.05$). The gene sets showing a 2-fold increase in expression after 2 days contain predominately categories belonging to secondary metabolism and metabolisms of polyketides and nonribosomal peptide synthesis, virulence, and siderophore-iron transport ($P < 0.001$) (see Data Set S2 in the supplemental material). The gene sets showing a 2-fold increase in expression after 5 days contain the category belonging to unclassified genes ($P < 0.01$) (see Data Set S2).

***F. verticillioides* gene clusters differentially expressed during cocultivation.** *F. verticillioides* gene clusters described in the whole genome annotation study (20) were investigated for coordinate expression during cocultivation. Three gene clusters of *F. verticillioides* show higher expression levels during cocultivation than

A

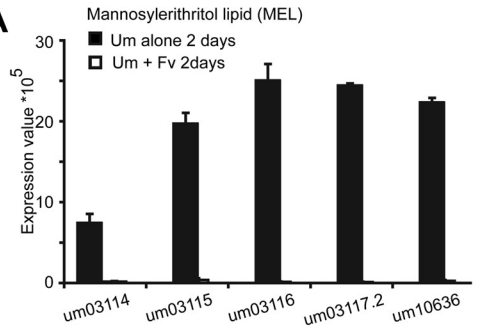

Locus ID	*gene*[1]	Putative function*
um03114	mat1	Acetyltransferase
um03115	mmf1	Major Facilitator
um03116	mac1	Acyltransferase
um03117.2	emt1	Erythritol-mannosyl-transferase
um10636	mac2	Acyltransferase

B

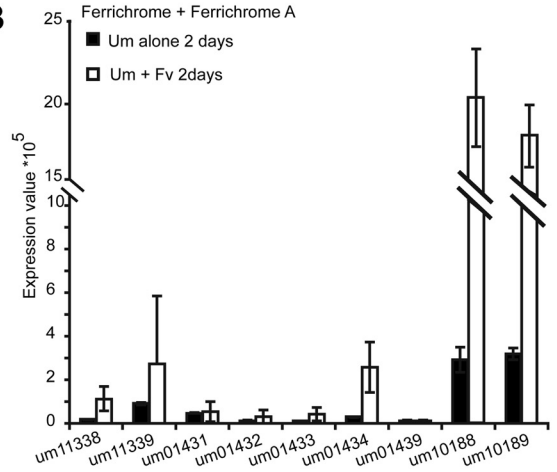

Locus ID	*gene*[2]	Putative function*
um11338	fer8	Dehydrogenase
um11339	fer7	Siderophore iron transporter 3
um01432	fer5	N6-hydroxylysine acetyl transferase
um01433	fer4	Enoyl-coa hydratase
um01434	fer3	Siderophore peptide synthetase
um01439	fer9	Related to fre3 - ferric reductase, reduces siderophore-bound iron prior to uptake
um10188	sid1	L-ornithine n5-oxygenase
um10189	sid2	Ferrichrome siderophore peptide synthetase

C

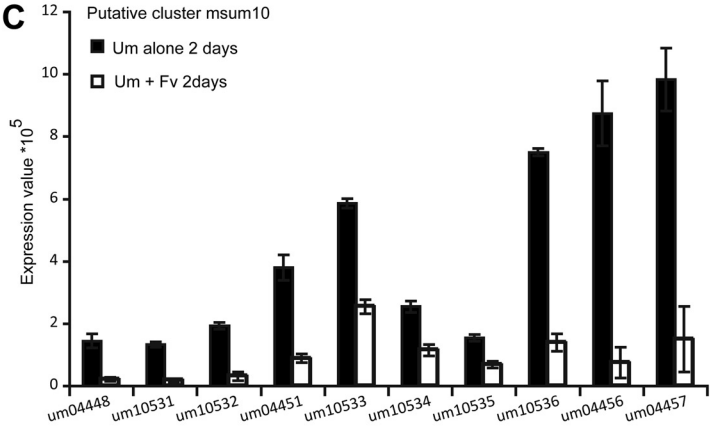

Locus ID	Putative function*
um04448	related to Myosin regulatory light chain 2-A, smooth muscle isoform
um10531	putative protein
um10532	related to polyketide synthase required for biosynthesis of fumonisin mycotoxins
um04451	conserved hypothetical protein
um10533	probable KGD1 – alpha-ketoglutarate dehydrogenase
um10534	related to Protein-tyrosine raminearum, receptor type 1
um10535	related to cell cycle control protein cwf15
um10536	related to FPR2 – FK506/rapamycin-binding protein of the ER
um04456	protein kinase A, catalytic subunit
um04457	conserved hypothetical protein

D

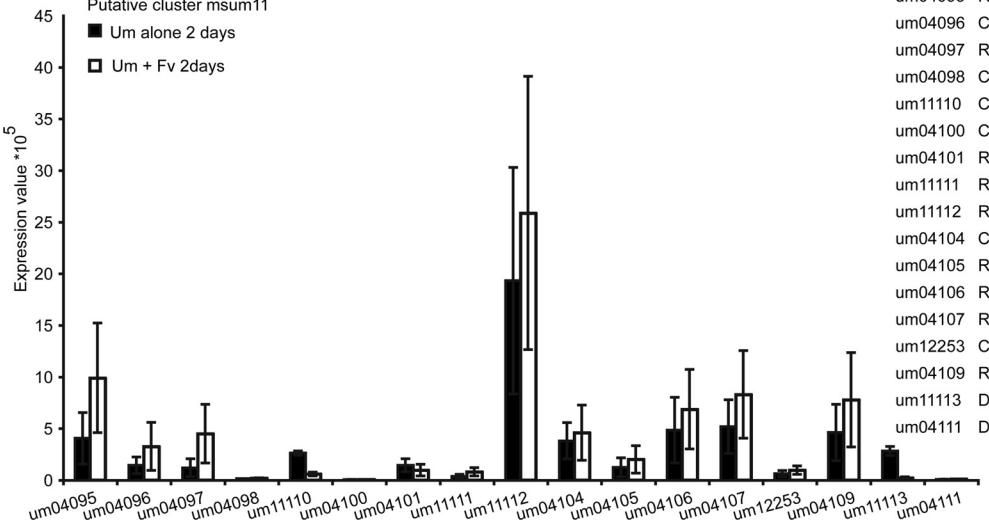

Locus ID	Putative function*
um04095	Related to polyketide synthase
um04096	Conserved hypothetical ustilago-specific protein
um04097	Related to polyketide synthase
um04098	Conserved hypothetical ustilago-specific protein
um11110	Conserved hypothetical protein
um04100	Conserved hypothetical ustilago-specific protein
um04101	Related to bas1 - transcription factor
um11111	Related to ascorbate oxidase precursor
um11112	Related to versicolorin b synthase
um04104	Conserved hypothetical ustilago-specific protein
um04105	Related to polyketide synthase
um04106	Related to o-methyltransferase b
um04107	Related to phenol 2-monooxygenase
um12253	Conserved hypothetical ustilago-specific protein
um04109	Related to cytochrome p450
um11113	Dehydrogenase
um04111	Dioxygenase

cultures of *F. verticillioides* grown alone at day 2 of growth. Cluster FV3_17 is involved in the biosynthesis of the metabolite fusarin C. It spans nine genes (FVEG_11078 to FVEG_11086; Fig. 6A) which are all specifically upregulated during cocultivation after 2 days (Fig. 6A).

Cluster FV3_5 contains 11 genes (FVEG_11927 to FVEG_11937; Fig. 6B) of which four (FVEG_11927, FVEG_11928, FVEG_11931, and FVEG_11932) are expressed more highly during cocultivation after 2 days compared to in growth alone (Fig. 6B).

The third cluster that shows higher gene expression at day 2 after cocultivation than growth of *F. verticillioides* alone (Fig. 6C) is cluster FV3_28. It spans seven genes (FVEG_12519 to FVEG_12525; Fig. 6C), of which five are specifically upregulated during cocultivation.

The identity of the metabolite produced by cluster FV3_5 is still unknown, but it has recently been shown that cluster FV3_28 is responsible for fusaric acid (FA) production (5). As speculated before, a PKS and an amino acid kinase are both involved in the production of FA (31) and cluster FV3_28 contains a reducing PKS gene (FVEG_12523) and a gene that encodes a protein similar to aspartokinase (FVEG_12521).

Cluster FV3_32 is specifically upregulated at day 5 when *F. verticillioides* is grown alone compared to that during cocultivation. This cluster spans eight genes (FVEG_05537 to FVEG_05544; Fig. 6D), of which seven are more highly expressed, and contains, among others, genes encoding a PKS, three cytochrome P450 enzymes, and a methyltransferase.

The cluster FV3_33 contains genes encoding enzymes that play a role in carotene synthesis and show specifically greater expression levels when grown alone compared to together, for both 2 and 5 days after inoculation. This suggests that cocultivation with *U. maydis* might inhibit carotene synthesis.

Cluster FV3_24 contains 4 genes, which all show greater expression at day 2 compared to at day 5 when *F. verticillioides* is grown alone as well as when grown together with *U. maydis*. This cluster contains genes encoding a PKS, an acyltransferase, and two predicted proteins of unknown function (Fig. 6F).

Other *F. verticillioides* genes differentially expressed during cocultivation. After 2 and 5 days, 60 and 137 genes, respectively, from *F. verticillioides* were more highly expressed (≥2-fold) during cocultivation with *U. maydis* than when grown alone (see Data Set S3 in the supplemental material). Thirteen of the 60 genes at day 2 and 53 genes of the 137 found at day 5 were annotated as proteins of unknown function. A BLASTp (1) search of the GenBank nonredundant database did not reveal any information on putative protein domains or domain functions associated with the predicted proteins.

Three *F. verticillioides* genes are found upregulated at both days 2 and 5: FVEG_08880, encoding a conserved predicted integral membrane protein; FVEG_07821, encoding a *Fusarium*-specific protein of unknown function; and FVEG_11867, which encodes a predicted glycosyl hydrolase family 5 protein.

Among the *F. verticillioides* genes with greater expression in cultures grown together with *U. maydis* than when grown alone are those encoding enzymes potentially directed toward microbial attachment and cell wall degradation. Genes encoding the cell wall-linked, glycophosphatidylinositol (GPI) anchor proteins expressed during the interaction between *F. verticillioides* and *U. maydis* may function to attach one fungus to the other. One such gene is more highly expressed after 2 days and six genes after 5 days of fungal cocultivation. Proteins involved in cell wall degradation include glycosyl hydrolases such as endo-chitinases as well as WSC (cell wall and stress response component) and LysM domain-containing proteins. Additionally, genes for a lipase and a hydrophobin were upregulated, and these compounds have the potential to confer the ability to adhere to, penetrate, or degrade microbial hydrophobic layers. Four such differentially regulated genes with potential wall-directed activity were detected after 2 days, and 14 were detected after 5 days. Interestingly, a hydrophobin gene in *U. maydis* was also found upregulated in coculture. The regulation of these genes in confronted cultures indicates that *F. verticillioides* may attach to and degrade the cell wall of *U. maydis*, a process that might contribute to the decline in *U. maydis* biomass that peaks after 5 days.

Other genes which might be involved in the degradation of *U. maydis* by *F. verticillioides* are the extracellular proteases and amino acid-degrading enzymes like serine proteases, carboxylesterases, and amidases. Genes for two such enzymes are more highly expressed after 2 days, and after 5 days, six genes in this category are upregulated.

Another group of proteins encoded by genes preferentially expressed during cocultivation of *F. verticillioides* and with *U. maydis* are transporters, permeases, and major facilitator proteins. Among these are Fst1, Fst2, Fst3, and Fst6 (FVEG_08441, FVEG_13078, FVEG_05690, and FVEG_10089, respectively). Fst1 is a putative sugar transporter, involved in the production of fumonisin B_1, and is important to the colonization of maize (14).

The gene sets showing 2-fold-higher expression were imported into the functional category (FunCat) database directory of MIPS (25) in order to determine if the genes differentially regulated during cocultivation are significantly enriched in particular gene categories compared to the genome as a whole ($P < 0.05$). Genes were assigned to functional categories based on the designation of their *Fusarium graminearum* ortholog, if present, using the FG3 annotation for the *F. graminearum* genome. After 2 days in confronted cultures, the categories of oxygen and radical detoxifica-

FIG 5 (A) Histogram of expression values of the genes from the MEL cluster in single and cocultivation cultures 2 days after inoculation. Black bars represent single-grown *U. maydis* samples and white bars the cocultivated *F. verticillioides* and *U. maydis* samples. The table on the right gives the gene names and functions for the encoded proteins found in the cluster. [1], gene and annotated function as mentioned previously (10). (B) Histogram of expression values of the genes from ferrichrome and ferrichrome A cluster in single and cocultivation cultures 2 days after inoculation. Black bars represent single-grown *U. maydis* samples and white bars the cocultivated *F. verticillioides* and *U. maydis* samples. The table on the right gives the gene names and functions of the encoded proteins found in the cluster. [2], gene and annotated function as mentioned previously (34). (C) Histogram of expression values of the *U. maydis* genes from putative cluster msum_10 (17) in single and cocultivation cultures 2 days after inoculation. Black bars represent single-grown *U. maydis* samples and white bars the cocultivated *F. verticillioides* and *U. maydis* samples. The table on the right gives the putative functions of the encoded proteins found in the cluster. (D) Histogram of expression values of the *U. maydis* genes from putative cluster msum_11 (17) in single and cocultivation cultures 2 days after inoculation. Black bars represent single-grown *U. maydis* samples and white bars the cocultivated *F. verticillioides* and *U. maydis* samples. The table on the right gives the putative functions of the encoding proteins found in the cluster. *, putative functions of the encoding proteins found in the cluster as determined by BLAST (1) if not already annotated.

A

Locus ID	Putative function*
FVEG_11078	Methyltransferase
FVEG_11079	Cytochrome p450 monooxygenase
FVEG_11080	Dehydrogenase
FVEG_11081	Major facilitator
FVEG_11082	Oxidoreductase
FVEG_11083	Aspartyl protease
FVEG_11084	Similar to elongation factor-1 gamma
FVEG_11085	Hydrolase
FVEG_11086	Pks FUSS

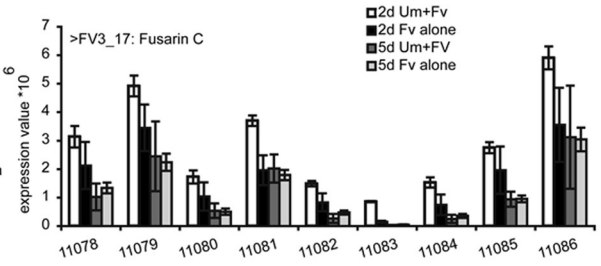

B

Locus ID	Putative function*
FVEG_11927	Unknown
FVEG_11928	Cytochrome p450 monooxygenase
FVEG_11929	Major facilitator
FVEG_11930	Major facilitator
FVEG_11931	Zinc-binding dehydrogenase
FVEG_11932	Polyketide synthase
FVEG_11933	Similar to beta-fructofuranosidase
FVEG_11934	Thioredoxin reductase, putative
FVEG_11935	Aminotransferase
FVEG_11936	Unknown
FVEG_11937	Similar to aspartate racemase

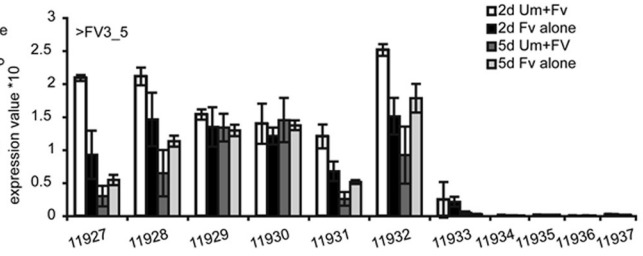

C

Locus ID	Putative function*
FVEG_12519	Homoserine o-acetyltransferase
FVEG_12520	Unknown
FVEG_12521	Aspartokinase
FVEG_12522	Unknown
FVEG_12523	Polyketide synthase
FVEG_12524	Carboxylesterase
FVEG_12525	Acyl-coa dehydrogenase

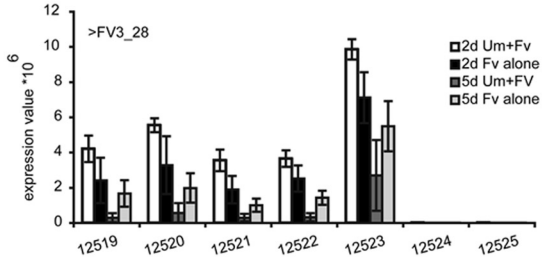

D

Locus ID	Putative function*
FVEG_05537	Polyketide synthase
FVEG_05538	Cytochrome p450 monooxygenase
FVEG_05539	Methyltransferase
FVEG_05540	Similar to extracellular lipase
FVEG_05541	Unknown
FVEG_05542	Cytochrome p450 monooxygenase
FVEG_05543	Unknown
FVEG_05544	Cytochrome p450 monooxygenase

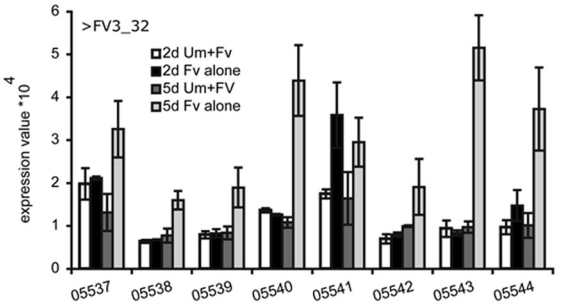

E

Locus ID	*gene*[1]	Putative function*
FVEG_10714		Ammonium transporter
FVEG_10715		High affinity methionine permease
FVEG_10716	*carO*	Opsin-like protein
FVEG_10717	*carB*	Phytoene dehydrogenase
FVEG_10718	*carRA*	Carotene cyclase
FVEG_10719	*carX*	Carotenoid oxygenase
FVEG_10720		$Zn(II)_2cys_6$ transcription factor
FVEG_10721		Dihydrodipicolinate synthetase
FVEG_10722		Oxidase

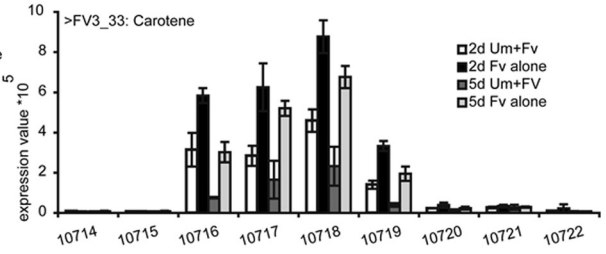

F

Locus ID	Putative function*
FVEG_00076	Unknown
FVEG_00077	Acyltransferase
FVEG_00078	Unknown
FVEG_00079	Polyketide synthase

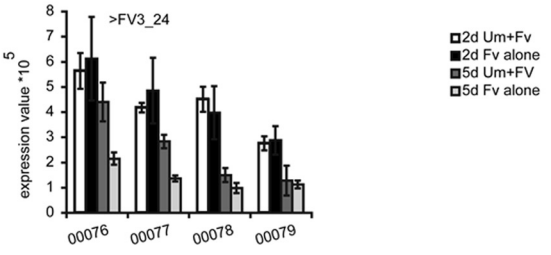

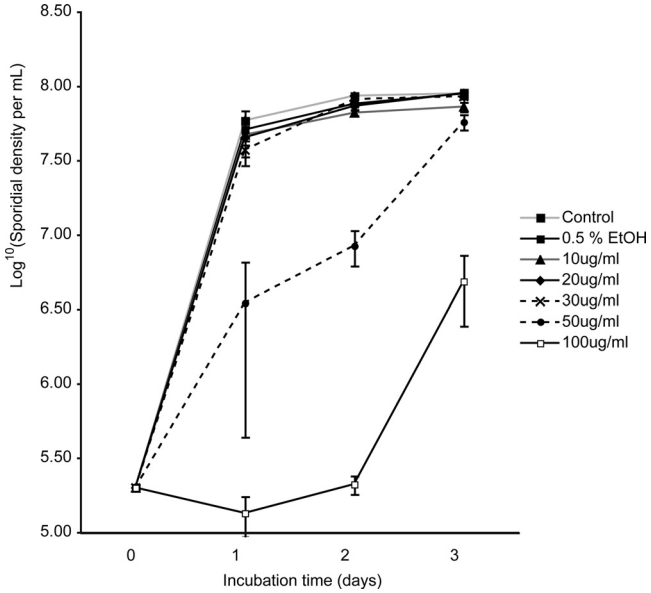

FIG 7 Growth curve of *U. maydis* after addition of different concentrations of fusaric acid. Solvent (0.5% ethanol) alone and small doses of 10, 20, and 30 μg/ml, represented by a solid black line with solid black squares, solid gray line with solid black triangles, solid black line with solid black diamonds, and dashed line with black crosses, respectively, do not show a decrease in growth of *U. maydis* compared to that of the untreated control (solid gray line with solid black squares). The two higher doses, 50 and 100 μg/ml, represented by a dashed black line with solid black circles and solid black line with white squares, respectively, result in significantly lower growth rates of *U. maydis*.

tion and detoxification in general are overrepresented in this data set ($P < 0.05$) (see Data Set S4 in the supplemental material). After 5 days in confronted cultures, the categories of amino acid metabolism and amino acid degradation and the category of virulence and disease factor are overrepresented in this data set ($P < 0.05$) (see Data Set S4).

Effect of fusaric acid on *U. maydis* growth. Since we found that *F. verticillioides* expresses increased transcript levels of fusaric acid biosynthesis genes and that the levels of the compound itself are elevated during cocultivation, we sought to determine the contribution of fusaric acid to the growth inhibition of *U. maydis* during this process. To do so, we added fusaric acid to *U. maydis* cultures and monitored fungal growth using a hemocytometer. Concentrations of 10, 20, or 30 μg/ml fusaric acid did not significantly reduce *U. maydis* growth, but higher concentrations of 50 and 100 μg/ml did (Fig. 7). These concentrations are in the range that fusaric acid is produced under similar conditions by *F. verticillioides* (data not shown). This result suggests that fusaric acid is an important compound produced by *F. verticillioides* contributing to *U. maydis* growth reduction during cocultivation.

DISCUSSION

In this report, *U. maydis* and *F. verticillioides* cultures were grown in liquid medium separately or together in order to study the dynamics of their interaction over time. Both fungi are found commonly in soil as well as in maize, and it has been shown that *F. verticillioides* can reduce disease severity caused by *U. maydis* (18). This study was intended to investigate their competition for nutrients as well as the direct antagonistic actions between the two in a controlled setting. Changes over time in biomass, metabolite accumulation, and gene expression patterns suggest mechanisms by which the fungi interact. Comparing fungal biomass that accumulates during cocultivation to that achieved in individually grown cultures and using qPCR measurements to assess relative amounts of each fungus, an increased growth rate was found during cocultivation over the first 2 days. These organisms thus may have mechanisms of sensing and responding to each other's presence, and the early growth spurt may potentially allow for a competitive advantage. Eventually, as inferred by reduced biomass and gene expression, *U. maydis* appears to be greatly inhibited and, based on gene expression analysis during the interaction, is maybe affected by *F. verticillioides* toxins and enzymes causing growth inhibition and perhaps direct cell death. Such a finding correlates well with our previous observations that *F. verticillioides* limits the growth of *U. maydis* both *in planta* (16, 17) and under different *in vitro* conditions (22). *F. verticillioides* also shows less growth at later time points in the presence of *U. maydis* than when grown alone, which may be due to self-inhibition or reduced levels of nutrients.

An example of a *U. maydis* counterresponse is the action of iron siderophores for sequestering iron and thus depleting levels available to *F. verticillioides*. This is inferred by the upregulation of siderophore biosynthetic genes. *U. maydis* upregulates certain multidrug transporters possibly to export toxic metabolites produced by *F. verticillioides. U. maydis* also possibly regulates some genes involved in secondary metabolite production, such as PKS genes, although no metabolic evidence for upregulation of toxin production by *U. maydis* was found. Further, we have observed that *U. maydis* likely initiates a defense response in the presence of *F. verticillioides* through elevated expression of genes encoding oxidoreductases, heat shock proteins, and hydrophobins. Particularly intriguing is the elevated expression of genes encoding proteins that are unique to *U. maydis* and to the *Ustilaginaceae* fungal family. Often, these are genes that are found in clusters containing effector proteins and are particularly associated with the biotrophic phase and tumor formation (13). While most of those proteins have no assigned function, some may play a role in defense against other microorganisms living in the plant, in this case *F. verticillioides*, rather than affecting the plant directly.

The *U. maydis* counter response might be limited through the shutdown of metabolites like ustilagic acid, MEL D, and two other uncharacterized metabolites. The biosurfactant ustilagic acid, which exhibits antifungal properties (32), is found in much lower levels during cocultivation than when *U. maydis* is grown alone, and the genes involved in UA production are expressed at much lower levels. The same is true for MEL D; although not found in the supernatant, transcripts of genes involved in MEL D biosyn-

FIG 6 (A to F) Histogram of expression values of the *F. verticillioides* genes from putative clusters FV3_17, FV3_5, FV3_28, FV3_32, FV3_33, and FV3_24, respectively (20), in single and cocultivation cultures 2 and 5 days after inoculation. White bars represent the cocultivated *F. verticillioides* and *U. maydis* samples and black bars represent single-grown *F. verticillioides* samples at day 2. Dark-gray bars represent the cocultivated *F. verticillioides* and *U. maydis* samples and light-gray bars single-grown *F. verticillioides* samples at day 5. The tables on the left give the putative functions of the encoding proteins found in each of the clusters. *, putative functions of the encoded proteins found in the cluster as determined by BLAST (1) if not already annotated. [1], gene names of four characterized carotene genes.

thesis were found in much higher levels in single cultures than in cocultivation. Whether *F. verticillioides* influences the transcription of these clusters in *U. maydis* is unknown. One possibility is that during the confrontation, *U. maydis* itself shifts transcriptional activities to express other genes. Another possibility is that *F. verticillioides* actively interferes with *U. maydis* transcription. Interestingly, decrease in ustilagic acid concentrations was also observed on solid PDA medium (23) using the same *F. verticillioides* strain used in this study, but concentrations increased when confronted with a different *F. verticillioides* strain, F17. This suggests that, if present, the ability to interfere with *U. maydis* transcription of UA cluster genes possibly varies with the *F. verticillioides* genotype.

The response of *F. verticillioides* to cocultivation with *U. maydis* is further illustrated by the elevated expression of genes encoding cell wall-degrading enzymes and proteases as well as oxidoreductases and hydrogenases. Additionally, elevated FA production and upregulated expression of the FA gene cluster by *F. verticillioides* occurs during cocultivation compared to those in axenic culture. We found in a separate experiment that FA in concentrations of 50 μg/ml and higher have a direct inhibitory effect on *U. maydis* growth. This suggests that FA plays an important role in the interaction of the two fungi and is consistent with the observation that the amount of FA produced by *F. verticillioides* strains may affect its interactions with *U. maydis in planta* (17). FA has also been shown to have an antimicrobial affect toward *Phytophthora* and other *Oomycetes* species as well (29).

Upregulation of the genes from the fusarin C cluster was also observed, although the corresponding metabolite was not observed, perhaps due to the extraction procedure. Fusarin C has been reported to act as a mutagen to mammalian cell lines (30) and may be toxic to other eukaryotes, like *U. maydis*.

In conclusion, we have identified potentially critical molecular interactions between two important plant- and soil-associated fungi on the transcriptomic and metabolomic levels. The outcome of the interaction measured is that *F. verticillioides* reduces the growth of *U. maydis*, which may explain the reduced pathogenic potential of *U. maydis* previously observed (18). However, growth of *F. verticillioides* in the presence of *U. maydis* is also reduced although to a much lower extent than that of *U. maydis*. The ability of *F. verticillioides* to shut down secretion of some defensive metabolites by *U. maydis* may allow *F. verticillioides* to outcompete *U. maydis*. The potential of *F. verticillioides* to inhibit growth and limit disease caused by *U. maydis* nevertheless may also benefit overall fitness of the smut fungus since the plant death rate also slows, extending the biotrophic lifespan of *U. maydis* (17).

ACKNOWLEDGMENTS

We thank Stephan Harvey and Thomas Krick from the Center for Mass Spectrometry and Proteomics at the University of Minnesota for their valuable technical assistance and Mark Holland for suggestions on the statistical analysis of the data. The Minnesota Supercomputing Institute is kindly acknowledged for computing resources and support.

This research was funded by the National Science Foundation grant (EF-0723451) awarded to Georgiana May and H. Corby Kistler.

REFERENCES

1. **Altschul SF, et al.** 1997. Gapped BLAST and PSI-BLAST: a new generation of protein database search programs. Nucleic Acids Res. **25**:3389–3402.
2. **Bacon CW, Hinton DM.** 1996. Symptomless endophytic colonization of maize by *Fusarium moniliforme.* Can. J. Bot. **74**:1195–1202.
3. **Basse CW, Boller T.** 1992. Glycopeptide elicitors of stress responses in tomato cells: N-linked glycans are essential for activity but act as suppressors of the same activity when released from the glycopeptides. Plant Physiol. **98**:1239–1247.
4. **Bolker M, Basse CW, Schirawski J.** 2008. *Ustilago maydis* secondary metabolism—from genomics to biochemistry. Fungal Genet. Biol. **45**(Suppl 1):S88–S93.
5. **Brown DW, Butchko RA, Baker SE, Proctor RH.** 2012. Phylogenomic and functional domain analysis of polyketide synthases in *Fusarium*. Fungal Biol. **116**:318–331.
6. **Dash S, Van Hemert J, Hong L, Wise RP, Dickerson JA.** 2012. PLEXdb: gene expression resources for plants and plant pathogens. Nucleic Acids Res. **40**:D1194–D1201.
7. **Decottignies A, et al.** 1995. Identification and characterization of SNQ2, a new multidrug ATP binding cassette transporter of the yeast plasma membrane. J. Biol. Chem. **270**:18150–18157.
8. **Felix G, Regenass M, Boller T.** 1993. Specific perception of subnanomolar concentrations of chitin fragments by tomato cells: induction of extracellular alkalinization, changes in protein phosphorylation, and establishment of a refractory state. Plant J. **4**:307–316.
9. **Granado J, Felix G, Boller T.** 1995. Perception of fungal sterols in plants (subnanomolar concentrations of ergosterol elicit extracellular alkalinization in tomato cells). Plant Physiol. **107**:485–490.
10. **Hewald S, et al.** 2006. Identification of a gene cluster for biosynthesis of mannosylerythritol lipids in the basidiomycetous fungus *Ustilago maydis*. Appl. Environ. Microbiol. **72**:5469–5477.
11. **Jones JD, Dangl JL.** 2006. The plant immune system. Nature **444**:323–329.
12. **Jumpponen A, Jones KL.** 2009. Massively parallel 454 sequencing indicates hyperdiverse fungal communities in temperate *Quercus macrocarpa* phyllosphere. New Phytol. **184**:438–448.
13. **Kamper J, et al.** 2006. Insights from the genome of the biotrophic fungal plant pathogen *Ustilago maydis*. Nature **444**:97–101.
14. **Kim H, Woloshuk CP.** 2011. Functional characterization of *fst1* in *Fusarium verticillioides* during colonization of maize kernels. Mol. Plant Microbe Interact. **24**:18–24.
15. **Kloppholz S, Kuhn H, Requena N.** 2011. A secreted fungal effector of *Glomus intraradices* promotes symbiotic biotrophy. Curr. Biol. **21**:1204–1209.
16. **Kornitzer D.** 2009. Fungal mechanisms for host iron acquisition. Curr. Opin. Microbiol. **12**:377–383.
17. **Lee K.** 2010. The effects of endophytic *Fusarium verticillioides* on the interactions of maize and its fungal pathogen, *Ustilago maydis*. Ph.D. dissertation. University of Minnesota, Minneapolis, MN.
18. **Lee K, Pan JJ, May G.** 2009. Endophytic *Fusarium verticillioides* reduces disease severity caused by *Ustilago maydis* on maize. FEMS Microbiol. Lett. **299**:31–37.
19. **Lee W.** 2010. Comprehensive discovery of fungal gene clusters: unexpected co-work reflected at the genomic level. Ph.D. dissertation. Technische Universität München, München, Germany.
20. **Ma L-J, et al.** 2010. Comparative genomics reveals mobile pathogenicity chromosomes in *Fusarium*. Nature **464**:367–373.
21. **Oliva R, et al.** 2010. Recent developments in effector biology of filamentous plant pathogens. Cell Microbiol. **12**:705–715.
22. **Pan JJ, Baumgarten AM, May G.** 2008. Effects of host plant environment and *Ustilago maydis* infection on the fungal endophyte community of maize (*Zea mays*). New Phytol. **178**:147–156.
23. **Rodriguez Estrada AE, Hegeman A, Kistler HC, May G.** 2011. *In vitro* interactions between *Fusarium verticillioides* and *Ustilago maydis* through real-time PCR and metabolic profiling. Fungal Genet. Biol. **48**:874–885.
24. **Rodriguez RJ, White JF, Jr, Arnold AE, Redman RS.** 2009. Fungal endophytes: diversity and functional roles. New Phytol. **182**:314–330.
25. **Ruepp A, et al.** 2004. The FunCat, a functional annotation scheme for systematic classification of proteins from whole genomes. Nucleic Acids Res. **32**:5539–5545.
26. **Rustici G, et al.** 2007. Global transcriptional responses of fission and budding yeast to changes in copper and iron levels: a comparative study. Genome Biol. **8**:R73.
27. **Saunders M, Kohn LM.** 2009. Evidence for alteration of fungal endophyte community assembly by host defense compounds. New Phytol. **182**:229–238.
28. **Schirawski J, et al.** 2010. Pathogenicity determinants in smut fungi revealed by genome comparison. Science **330**:1546–1548.
29. **Son SW, et al.** 2008. Bikaverin and fusaric acid from *Fusarium oxysporum*

show antioomycete activity against *Phytophthora infestans*. J. Appl. Microbiol. **104**:692–698.
30. **Sondergaard TE, et al.** 2011. Fusarin C acts like an estrogenic agonist and stimulates breast cancer cells *in vitro*. Toxicol. Lett. **205**:116–121.
31. **Stipanovic RD, et al.** 2011. Nuclear magnetic resonance (NMR) studies on the biosynthesis of fusaric acid from *Fusarium oxysporum* f. sp. *vasinfectum*. J. Agric. Food Chem. **59**:5351–5356.
32. **Teichmann B, Linne U, Hewald S, Marahiel MA, Bolker M.** 2007. A biosynthetic gene cluster for a secreted cellobiose lipid with antifungal activity from *Ustilago maydis*. Mol. Microbiol. **66**:525–533.
33. **van den Hazel HB, et al.** 1999. PDR16 and PDR17, two homologous genes of *Saccharomyces cerevisiae*, affect lipid biosynthesis and resistance to multiple drugs. J. Biol. Chem. **274**:1934–1941.
34. **Winterberg B, et al.** 2010. Elucidation of the complete ferrichrome A biosynthetic pathway in *Ustilago maydis*. Mol. Microbiol. **75**:1260–1271.